Radiative Corrections to Electron-Proton Scattering*

YUNG-SU TSAI
Institute of Theoretical Physics, Department of Physics, Stanford University, Stanford, California
(Received November 15, 1960)

The radiative corrections to the electron-proton scattering are calculated with the effects of the proton recoil taken into account. We assumed the experimental conditions of Hofstadter *et al.* at Stanford, namely only the final electrons are momentum-analyzed. The anisotropy in the maximum energy of photons which can be emitted and the radiation from the proton current are the two main effects due to the proton recoil, and both effects are considered. The mesonic effects in the two-photon exchange diagrams are not considered. Other than the uncertainty in the mesonic effects, our formula is good up to about 5 Bev.

I. INTRODUCTION

RECENTLY[1-4] the energy of the electron-proton scattering has been increased to around 1 Bev and within a few years the energy will probably go up to 5 Bev (Cambridge Machine) or 15 Bev (Stanford Monster). The purpose of this paper is to calculate the quantum electrodynamic parts of the radiative corrections which are applicable up to 5 Bev of the incident energy.

Schwinger[5] first calculated the radiative corrections to the potential scattering and he found that the cross section is altered by a factor $(1+\delta)$, where

$$\delta\approx\frac{-2\alpha}{\pi}\left\{\left(\ln\frac{E}{\Delta E}-\frac{13}{12}\right)\left(\ln\frac{-q^2}{m^2}-1\right)+\frac{17}{36}\right\}. \quad \text{(I.1)}$$

Here q is the four-momentum transfer, E is the energy of incident or scattered electrons (in the potential scattering they are identical), m is the rest mass of the electron, and ΔE is the maximum energy loss of the electron or the maximum energy of a photon which can be emitted (they are identical in the potential scattering). In the region $M^2\gg-q^2\gg m^2$, where M is the rest mass of the proton, Eq. (I.1) is a good approximation and has been used extensively by the experimentalists[6] in analyzing the data of the e–p scattering. However at high incident energy and large scattering angle, i.e., $-q^2\gtrsim M^2$, the incident energy (E_1) is no longer equal to the energy of the final electron (E_3) and the maximum energy loss of the electron ΔE is no longer equal to the maximum energy of a photon which can be emitted. In fact E_3 and E_1 are related by the formula

$$E_3=E_1/\eta, \quad \text{(I.2)}$$

where

$$\eta\equiv 1+E_1M^{-1}(1-\cos\theta). \quad \text{(I.3)}$$

For definiteness let us define the energy resolution ΔE as the experimental quantity shown in Fig. 1. Then from the energy-momentum conservation, it can be shown that the maximum energy of a photon which can be emitted along the direction of the final electron is ΔE, but in the direction of the incident electron it is $\eta^2\Delta E$. Thus Eq. (I.1) becomes quite ambiguous in the practical application at high energies because one does not know what to use for E and ΔE. Intuitively one would guess that Eq. (I.1) should be changed to

$$\delta\approx\frac{-2\alpha}{\pi}\left\{\left(\frac{1}{2}\ln\frac{E_1}{\eta^2\Delta E}+\frac{1}{2}\ln\frac{E_3}{\Delta E}-\frac{13}{12}\right)\times\left(\ln\frac{-q^2}{m^2}-1\right)+\frac{17}{36}\right\}. \quad \text{(I.4)}$$

It will be shown later that Eq. (I.4) is approximately true if one neglects the radiation by the proton current.

When $-q^2\gtrsim M^2$ the velocity of the recoil proton v_4 approaches the velocity of light, i.e., $\beta_4\equiv v_4/c\to 1$. Thus one would expect that in this case the radiation

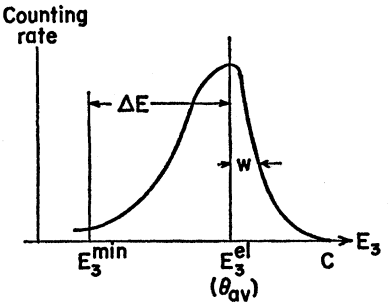

FIG. 1. A typical energy spectrum of the scattered electrons at a fixed angle. The point $E_3^{el}(\theta_{av})$ is chosen to be the energy of the elastically scattered electron at the center of the entrance slit. ΔE should be chosen such that $W\ll\Delta E\ll E_3(1+2E_1/M)^{-1}$. The widths W is caused by the energy spread in the incident beam and the finite width of the entrance slit. The curve should be integrated from E_3^{min} to C in order to compute the cross section.

* Supported in part by the U. S. Air Force through the Air Force Office of Scientific Research.

[1] R. Hofstadter and R. R. Wilson, *Proceedings of the Tenth Annual International Conference on High-Energy Physics at Rochester* (Interscience Publishers, Inc., New York, 1960).

[2] L. N. Hand, Phys. Rev. Letters **5**, 168 (1960).

[3] F. Bumiller, M. Croissiaux, and R. Hofstadter, Phys. Rev. Letters **5**, 261 (1960); **5**, 263 (1960).

[4] R. R. Wilson, K. Berkelman, and J. Cassels, Cornell University reprint (to be published).

[5] J. Schwinger, Phys. Rev. **76**, 760 (1949), Eq. (2.105).

[6] R. Hofstadter, Revs. Modern Phys. **28**, 214 (1956). Actually the energy of the scattered electron E_3 was used in E of Eq. (I.1) in this reference.

from the proton current would be no longer negligible. If one tries to calculate the bremsstrahlung from the proton current, one encounters the usual infrared divergence and thus one is forced to consider diagrams such as M_2, M_3, and M_6 in Fig. 2 in order to achieve the infrared cancellation. The exact calculation of M_2, M_3, and M_6 is not attempted in this paper since to do it one has to consider mesonic contributions from these diagrams such as carried out by Drell and Fubini.[7] We shall merely extract the infrared contributions from these diagrams using the technique developed by Yennie, Frautschi, and Suura.[8]

It has been emphasized by the present author[9] in a previous paper that in the calculation of the radiative corrections for any process a critical analysis of the experimental corrections for any process a critical analysis of the experimental conditions is necessary. We shall proceed to discuss our problem in the same spirit. The experimental conditions assumed are those of Hofstadter *et al.* at Stanford that electrons, after being scattered by a hydrogen target and going through an entrance slit, are momentum analyzed by a magnetic spectrometer and the recoil protons are left undetected.

The notation used is similar to that in reference 9. p_1 and p_3 represent the four-momenta of incident and scattered electrons, respectively. p_2 and p_4 are the four-momenta of initial and recoil protons, respectively. The metric chosen is such that $p_1\cdot p_2=E_1E_2-\mathbf{p}_1\cdot\mathbf{p}_2$. The units $\hbar=c=1$ and $e^2/4\pi=\alpha$ are used. $\not{p}$ represents $p_\mu\gamma_\mu$.

The infrared divergence is avoided by assuming that a photon has a small fictitious mass λ whenever we encounter integrations in which such divergence occurs. When the photon mass λ is used, it always appears in both the elastic and inelastic cross sections in the form[10]

$$K(p_i,p_j)\equiv(p_i\cdot p_j)\int_0^1\frac{dy}{p_y^2}\ln\frac{p_y^2}{\lambda^2},\qquad\text{(I.5)}$$

where $p_y=p_iy+p_j(1-y)$. We shall call terms of this kind infrared terms. They always cancel out completely when elastic and inelastic cross sections are added together. Thus one does not have to integrate Eq. (I.5) explicitly. [In the matrix element of M_2 of Fig. 2, we shall see that the infrared terms have the form $K(p_i,-p_j)$ instead of $K(p_i,p_j)$. $K(p_i,-p_j)$ is complex. In our calculation only the real part of M_2 contributes to the cross section, and it can be shown[8] that

$$\mathrm{Re}\,K(p_i,-p_j)\approx K(p_i,p_j).]$$

Terms of order $m^2/-q^2$ compared with unity are neglected throughout in this paper. In the calculation of the contribution to the cross section by the radiation from the proton current one encounters a lot of Spence functions $\Phi(x)$. We shall neglect those Spence functions which are of order unity, e.g., $\Phi(1)$. This approximation causes an error of order $\alpha\approx1\%$ in the cross section.

In Secs. II and III elastic and inelastic scattering cross sections, respectively, are treated. The observable cross section is obtained by adding elastic and inelastic cross sections. In Sec. IV some numerical examples are given. In Sec. V some precautions to the practical applications of our formula are considered.

II. ELASTIC SCATTERING CROSS SECTION

The Feynman diagrams contributing to the elastic scattering cross section to order α^3 are shown in Fig. 2. The expression for the elastic scattering cross section can be written as[11]

$$d\sigma_{\text{elastic}}=(2\pi)^2\frac{E_1E_2}{[(p_1p_2)^2-m^2M^2]^{\frac{1}{2}}}\times\frac{1}{4}\int\delta(p_3+p_4-p_1-p_2)d^3p_3d^3p_4\times\sum_{\text{spin}}\Big[M_1^\dagger M_1+\sum_{i=2}^{6}2\,\mathrm{Re}(M_1^\dagger M_i)\Big].\qquad\text{(II.1)}$$

The first term in the square bracket of Eq. (II.1) represents the Rosenbluth cross section. The matrix

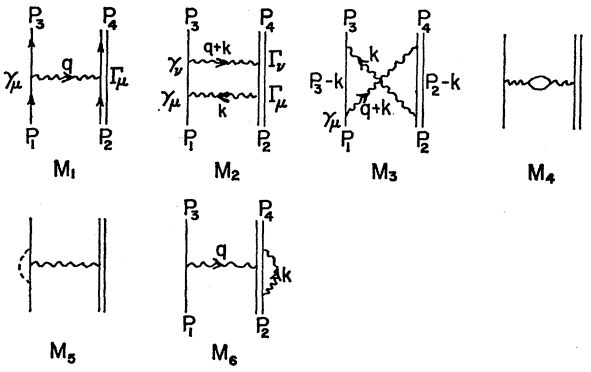

FIG. 2. Feynman diagrams for elastic scattering.

[7] S. D. Drell and S. Fubini, Phys. Rev. **113**, 741 (1959).

[8] D. R. Yennie, S. C. Frautschi, and H. Suura, Ann. Phys. (to be published). In addition to the problem of infrared divergence these authors also gave a general treatment of the recoil effects in the electron-proton scattering. The purpose of our paper is to derive a convenient formula which can be used readily by the experimentalists. Thus the present work and these authors' work are complementary to each other.

[9] Y. S. Tsai, Phys. Rev. **120**, 269 (1960), also *Proceedings of the Tenth Annual International Conference on High-Energy Physics at Rochester* (Interscience Publishers, New York, 1960).

[10] The notations for the infrared terms are improved in this paper. $-2K(p_1,p_3)/q^2$ corresponds to $\mu_2(q^2)$ in reference 9.

[11] Compare with Eq. (1) of reference 9.

element M_1 can be written as[12]

$$M_1=\frac{-i\alpha Z}{\pi}\frac{mM}{(E_1E_2E_3E_4)^{\frac{1}{2}}}\frac{1}{q^2}\bar{u}(p_3)\gamma_\mu u(p_1)\bar{u}(p_4)\Gamma_\mu(q^2)u(p_2),$$

where $q=(p_1-p_3)$,

$$\Gamma_\mu(q^2)=F_1(q^2)\gamma_\mu+\frac{\kappa}{2M}F_2(q^2)\boldsymbol{q}\gamma_\mu, \qquad \text{(II.2)}$$

and $\kappa=1.79$ is the Pauli magnetic moment of the proton. $F_1(q^2)$ and $F_2(q^2)$ are the electric and magnetic form factors, respectively, of the proton and are to be determined by the experiment. After averaging over the initial states and summing over the final states, one obtains the Rosenbluth cross section[13]:

$$\left(\frac{d\sigma}{d\Omega}\right)_{\text{Rosenbluth}}=\frac{r_0^2m^2Z^2}{4E_1^2\eta}\frac{\cos^2(\theta/2)}{\sin^4(\theta/2)}$$
$$\times\left\{F_1^2-\frac{q^2}{4M^2}[2(F_1+\kappa F_2)^2\tan^2(\theta/2)+\kappa^2F_2^2]\right\}, \qquad \text{(II.3)}$$

where $r_0=\alpha m^{-1}\sim 2.82\times10^{-13}$ cm is the classical radius of an electron. For the vacuum polarization (M_4) and the electron vertex (M_5) diagrams, we can directly use the results of the electron-electron scattering calculation[14] and obtain

$$M_4=\frac{\alpha}{\pi}\left[\frac{-5}{9}+\frac{1}{3}\ln\left(\frac{-q^2}{m^2}\right)\right]M_1, \qquad \text{(II.4)}$$

$$M_5=-\frac{\alpha}{2\pi}[K(p_1,p_3)-K(p_1,p_1)-\tfrac{3}{2}\ln(-q^2/m^2)+2]M_1, \qquad \text{(II.5)}$$

where

$$K(p_i,p_j)=(p_i\cdot p_j)\int_0^1\frac{dy}{p_y^2}\ln\frac{p_y^2}{\lambda^2}, \quad p_y=p_iy+p_j(1-y).$$

The terms $K(p_1,p_3)$ and $K(p_1,p_1)$ in Eq. (II.5) are infrared terms. It will be shown later that they cancel out completely with the similar terms in the inelastic cross section and therefore they need not be integrated explicitly.

As mentioned in the previous section, we shall merely extract the infrared terms from M_2, M_3, and M_6 and assume the noninfrared parts of these diagrams to be negligible. Let us consider the matrix element for M_2 as shown in Fig. 2. When either of the 4-momenta of the photon propagators approaches zero, i.e., $k\to0$ or $k+q\to0$, we have infrared divergence. Suppose $k\to0$, then Γ_μ in M_2 of Fig. 2 can be replaced by γ_μ, and we may write the matrix element for M_2 as

$$M_2=\frac{e^4}{(2\pi)^6}\frac{mMZ^2}{(E_1E_2E_3E_4)^{\frac{1}{2}}}\int d^4k\,\bar{u}(p_3)\gamma_\nu\frac{\boldsymbol{p}_1+\boldsymbol{k}+m}{k^2+2p_1\cdot k}$$
$$\times\gamma_\mu u(p_1)\bar{u}(p_4)\Gamma_\nu\frac{\boldsymbol{p}_2-\boldsymbol{k}+M}{k^2-2k\cdot p_2}\gamma_\mu u(p_2)$$
$$\times\frac{1}{(k^2-\lambda^2)[(k+q)^2-\lambda^2]}. \qquad \text{(II.6)}$$

The infrared contribution from M_2 due to $k\to0$ is obtained by neglecting k in the numerator and in $(k+q)^2$, and we obtain

$$M_2'=\frac{i\alpha Z}{4\pi^3}\int\frac{4(p_1\cdot p_2)d^4k}{(k^2+2p_1\cdot k)(k^2-2k\cdot p_2)(k^2-\lambda^2)}M_1$$
$$=\frac{-\alpha Z}{2\pi}K(p_2,-p_1)M_1. \qquad \text{(II.7)}$$

Similarly the infrared contribution from M_2 due to $k+q\to0$ can be obtained by a substitution $k+q\to k$ in Eq. (II.6), and we have

$$M_2''=\frac{-\alpha Z}{2\pi}K(p_4,-p_3)M_1. \qquad \text{(II.8)}$$

Thus we have accomplished the extraction of infrared terms from M_2. Neglecting the noninfrared terms in M_2, we obtain

$$M_2=M_2'+M_2''$$
$$=\frac{-\alpha Z}{2\pi}M_1[K(p_2,-p_1)+K(p_4,-p_3)]. \qquad \text{(II.9)}$$

$K(p_2,-p_1)$ and $K(p_4,-p_3)$ are complex. Only the real parts contribute to the cross section. It can be shown that[8]

$$\text{Re}\,K(p_i,P_j)=K(p_i,p_j)+\text{"negligible,"} \qquad \text{(II.10)}$$

where "negligible" means the term of order unity. Using a similar method, one can extract the infrared terms from M_3. Neglecting the noninfrared terms in M_3, we get

$$M_3=\frac{\alpha Z}{2\pi}M_1[K(p_2,p_3)+K(p_4,p_1)]. \qquad \text{(II.11)}$$

Similarly, for M_6 we have

$$M_6=\frac{-\alpha Z^2}{2\pi}M_1[K(p_2,p_4)-K(p_2,p_2)], \qquad \text{(II.12)}$$

[12] Although we are primarily interested in the electron-proton scattering in this paper, our result can be used in the electron-nucleus scattering. The atomic number Z is kept here for this purpose. Also we shall see later that Z is a convenient quantity for identifying the contributions from various diagrams in the inelastic cross section. For electron-nucleus scattering the definitions of F_1, F_2, κ, and M should be appropriately changed.

[13] M. N. Rosenbluth, Phys. Rev. **79**, 615 (1950).

[14] See Eqs. (5) and (6) of reference 9.

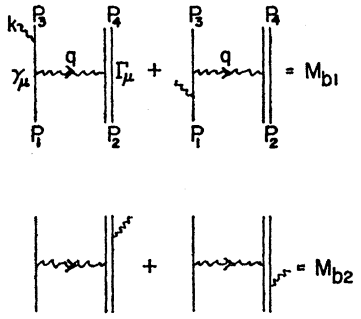

FIG. 3. Feynman diagrams for inelastic scattering.

where the term $K(p_2,p_2)$ was introduced by the renormalization of M_6 and represents the infrared term of the electromagnetic proton self-energy. [Compare Eq. (II.12) with Eq. (II.5).]

Substituting expressions for the matrix elements in Eq. (II.1), we obtain the elastic scattering cross section

$$\left(\frac{d\sigma}{d\Omega}\right)_{\text{elastic}}=\left(\frac{d\sigma}{d\Omega}\right)_{\text{Rosenbluth}}\left\{1+\frac{\alpha}{\pi}[-K(p_1,p_3)+K(p_1,p_1)-ZK(p_2,p_1)-ZK(p_4,p_3)+ZK(p_2,p_3)+ZK(p_4,p_1)-Z^2K(p_2,p_4)+Z^2K(p_2,p_2)]+\frac{\alpha}{\pi}\left[\frac{-28}{9}+\frac{13}{6}\ln\frac{-q^2}{m^2}\right]\right\}. \quad \text{(II.13)}$$

III. INELASTIC CROSS SECTION

The Feynman diagrams for the matrix elements contributing to the inelastic cross section to order α^3 are shown in Fig. 3. Since we are interested only in the soft photon emissions, the vertex function connecting the real photon k and the proton current may be approximated by γ_ν. Thus the matrix elements M_{b1} and M_{b2} may be written as

$$M_{b1}=\frac{e^3}{(2\pi)^{7/2}}\frac{mMZ}{(2\omega E_1E_2E_3E_4)^{\frac{1}{2}}}\bar{u}(p_3)\left[e\frac{p_3+k+m}{2p_3\cdot k}\gamma_\mu-\gamma_\mu\frac{p_1-k+m}{2p_1\cdot k}e\right]u(p_1)\bar{u}(p_4)\Gamma_\mu u(p_2)\times[1/(p_1-p_3-k)^2], \quad \text{(III.1)}$$

$$M_{b2}=\frac{-e^3}{(2\pi)^{7/2}}\frac{mMZ^2}{(2\omega E_1E_2E_3E_4)^{\frac{1}{2}}}\bar{u}(p_3)\gamma_\mu u(p_1)\times\bar{u}(p_4)\left[e\frac{p_4+k+M}{2p_4\cdot k}\Gamma_\mu-\Gamma_\mu\frac{p_2-k+M}{2p_2\cdot k}e\right]\frac{u(P_2)}{(p_1-p_3)^2}. \quad \text{(III.2)}$$

We shall neglect the k's in the numerators of the above equations and in the term (p_1-p_3-k) in Eq. (III.1). The experimental conditions under which this approximation is valid will be discussed in detail in Appendix A. Here we simply state the result:

$$\Delta E(1+2E_1/M)\ll E_3. \quad \text{(III.3)}$$

With this approximation we may write

$$M_{b1}+M_{b2}\approx\frac{i}{\pi^2}\left(\frac{\alpha}{2}\right)^{\frac{1}{2}}M_1\frac{1}{(2\omega)^{\frac{1}{2}}}\times\left[\frac{p_3\cdot e}{p_3\cdot k}-\frac{p_1\cdot e}{p_1\cdot k}-\frac{Zp_4\cdot e}{p_4\cdot k}+\frac{Zp_2\cdot e}{p_2\cdot k}\right]. \quad \text{(III.4)}$$

The inelastic scattering cross section can be calculated by using the formula

$$d\sigma_b=(2\pi)^2\frac{E_1E_2}{[(p_1\cdot p_2)^2-m^2M^2]^{\frac{1}{2}}}\frac{1}{4}\int d^3p_3d^3p_4d^3k\times\delta(p_3+p_4+k-p_1-p_2)\times\sum_{\text{spin}}(M_{b1}^\dagger+M_{b2}^\dagger)(M_{b1}+M_{b2}). \quad \text{(III.5)}$$

In the above formula, one has to perform the integration

$$A=\int\frac{d^3p_3}{E_3}\int\frac{d^3k}{2\omega}\int\frac{d^3p_4}{E_4}\delta(p_3+p_4+k-p_1-p_2)\chi^2, \quad \text{(III.6)}$$

where

$$\chi^2=\left[\frac{p_3}{p_3\cdot k}-\frac{p_1}{p_1\cdot k}-\frac{Zp_4}{p_4\cdot k}+\frac{Zp_2}{p_2\cdot k}\right]^2. \quad \text{(III.7)}$$

The range of this integration is determined by the experimental conditions. One can perform this integration in any coordinate system provided the experimental conditions are transformed into those in the coordinate system in which the integration is carried out.[15] The procedure we shall use here is somewhat involved. In Stanford experiments k and p_4 are undetected and for p_3 the entrance slit and the spectrometer determine the angular range $(\theta_{\min},\theta_{\max})$ and the energy range $E_3>E_3^{\min}$, respectively. This experimental condition is shown in Fig. 4. The curve AD corresponds to the energy-angle relation of the elastically scattered electron obtained from Eq. (I.2). Only the electrons which are scattered into the area $ABCD$ are detected. As mentioned in the introduction, due to the recoil effect the maximum energy of a photon which can be emitted is very anisotropic. Very roughly speaking, the maximum energy of a photon which can be emitted in the forward direction is much larger than the maximum energy of a photon which can be emitted in the backward direction when there is a big recoil. Thus

[15] For choice of the coordinate system when Eq. (III.3) is not satisfied see Sec. VII.c of reference 9.

one has to perform the k integration in Eq. (III.6) in a very elongated ellipsoidal volume. We avoid doing this by choosing a special Lorentz frame in which this ellipsoid becomes a sphere and do the k integration in this frame. We then transform everything back into the laboratory system and use some other trick to do the p_3 integration. The p_4 integration is eliminated at the beginning by using the δ function. We will show more precisely in the following how this is done.

We first perform the p_4 integration by using the δ function and obtain

$$A=\int\frac{d^3p_3}{E_3}\int\frac{d^3k}{\omega}S(E_4)\delta((t-k)^2-M^2)\chi^2, \quad \text{(III.8)}$$

where

$$t\equiv p_4+k+p_1+p_2-p_3, \quad \text{(III.9)}$$

and

$$S(y)=1, \quad y>0$$
$$=0, \quad y<0.$$

In the special frame[16] $\mathbf{p}_4+\mathbf{k}=0$ or $t=(t_0,0)$, the δ function in Eq. (III.8) is independent of the angle in which the photon is emitted. Thus we perform the photon integration in this special frame:

$$A=\int d\Omega\int_{E_{\min}}^{E_{\max}}p_3dE_3\frac{[(kt)^2-\lambda^2t^2]^{\frac{1}{2}}}{2t^2}\times S(t^2-t_{\min}{}^2)\int d\tilde{\Omega}_k\chi^2, \quad \text{(III.10)}$$

where

$$t_{\min}{}^2=M^2+2M\lambda+\lambda^2\approx M^2+2M\lambda, \quad \text{(III.11)}$$

and the tilde represents the quantity in the special frame. After the photon angular integration, we transform all the quantities in the special frame back into those of the laboratory system and perform the p_3 integration. For the p_3 integration we use the following trick. From Eq. (III.9) we obtain

$$x\equiv t^2-M^2=2m^2+2M(E_1-E_3)-2E_1E_3(1-\cos\theta). \quad \text{(III.12)}$$

Thus instead of integrating with respect to E_3 and θ, we can integrate with respect to x and θ. Equation (III.10) can then be written as

$$A=\int d\Omega\frac{E_3}{4M\eta}\int_{x_{\min}}^{x_{\max}}\frac{xdx}{2(x+M)^2}\int d\tilde{\Omega}_k\chi^2, \quad \text{(III.13)}$$

where $x_{\min}=2\lambda M$, which corresponds to the value of x along the curve CD in Fig. 4, and $x_{\max}$ is the value of x along BC. The infrared divergence occurs just under the curve AD. Since relatively few electrons are scattered near the curve BC, we may replace the curve BC by $B'C'$ where the curve $B'C'$ is obtained by

$$x=x_{\max}\equiv 2m^2+2M(E_1-E_3{}^{\min})-2E_1E_3{}^{\min}(1-\cos\theta_{\rm av})\approx 2M\eta\Delta E, \quad \text{(III.14)}$$

where

$$\theta_{\rm av}\equiv(\theta_{\max}+\theta_{\min})^{\frac{1}{2}},$$
$$\Delta E\equiv E_3{}^{\rm el}(\theta_{\rm av})-E_{\min}, \quad \text{(III.15)}$$

and

$$E_3{}^{\rm el}(\theta_{\rm av})=\frac{E_1}{1+E_1M^{-1}(1-\cos\theta_{\rm av})}. \quad \text{(III.16)}$$

With this modification of the region of integration, $x_{\max}$ is now independent of θ, thus we can finally write

$$A=d\Omega\frac{E_3}{4M\eta}\int_{2M\lambda}^{2M\eta\Delta E}\frac{xdx}{2(x+M^2)}\int d\tilde{\Omega}_k\chi^2. \quad \text{(III.17)}$$

Using Eqs. (II.3), (III.5), and (III.17), we can express the inelastic scattering cross section as

$$\left(\frac{d\sigma}{d\Omega}\right)_b=-\left(\frac{d\sigma}{d\Omega}\right)_{\rm Rosenbluth}\frac{\alpha}{8\pi^2}\int_{2\lambda M}^{2M\eta\Delta E}\frac{xdx}{2(x+m^2)}\times\int d\tilde{\Omega}_k\chi^2. \quad \text{(III.18)}$$

The photon angular integration can be carried out in the following way:[17]

$$\begin{aligned}\int d\tilde{\Omega}_k\frac{(p_i\cdot p_j)}{(p_i\cdot k)(p_j\cdot k)}&=(p_i\cdot p_j)\int_0^1dy\int\frac{d\tilde{\Omega}_k}{(p_y\cdot k)^2}\\&=4\pi(p_i\cdot p_j)\int_0^1\frac{dy}{|\tilde{k}|^2p_y{}^2+\lambda^2E_y{}^2}\\&=4\pi(p_i\cdot p_j)\int_0^1\frac{t^2dy}{[(k\cdot t)^2-\lambda^2t^2]p_y{}^2+\lambda^2[(p_i\cdot t)y+(1-y)(p_j\cdot t)]^2}\\&=16\pi(p_i\cdot p_j)\int_0^1\frac{(x+M^2)dy}{(x^2-4\lambda^2M^2)p_y{}^2+4\lambda^2(p_j\cdot t)^2[1+y(p_i\cdot t-p_j\cdot t)(p_j\cdot t)^{-1}]^2}, \quad \text{(III.19)}\end{aligned}$$

[16] This coordinate system is often used in the calculation of processes in which two of the three final particles are undetected; for example, $\mu\to e+\nu+\nu$ or $e+p\to e+p+\pi$.

[17] *Note added in proof.* Strictly speaking, this angular integration is incorrect when $i=j=4$, since $p_4\cdot k=(x-\lambda^2)/2$ and is independent of photon direction. However, it can be shown that the same result is obtained by using the correct method as long as one considers only the emission of a soft photon.

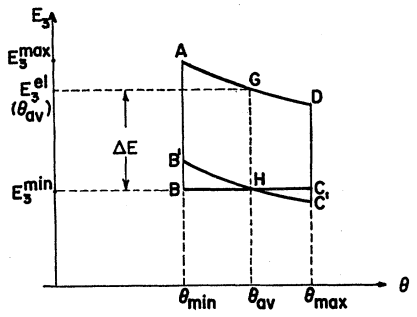

FIG. 4. θ_{min} and θ_{max} define the width of the entrance slit. E_3^{min} defines the spectrometer threshold. The curve AD corresponds to the elastic scattering. Only those electrons going into the area $ABCD$ are detected. We approximate the number of electrons going into the area $ABCD$ by the number of electrons going into the area $AB'C'C$.

where $p_y=p_i y+p_j(1-y)$. We have made the quantities in the special frame covariant by using $\tilde{\omega}=(k\cdot t)/(t^2)^{\frac{1}{2}}$, $\tilde{E}_i=(p_i\cdot t)/(t^2)^{\frac{1}{2}}$, and $(k\cdot t)=\frac{1}{2}(x+\lambda^2)$. Notice that the quantities $(p\cdot t)$ in Eq. (III.19) are important only in the infrared limit and therefore we can replace t by p_4, and we can express them in terms of lab quantities as follows:

$$p_1\cdot t\rightarrow ME_3,\quad p_2\cdot t\rightarrow ME_4,\qquad p_3\cdot t\rightarrow ME_1,\quad p_4\cdot t\rightarrow M^2. \tag{III.20}$$

The integration with respect to x can be carried out easily and we obtain

$$\int_{2\lambda M}^{2M\eta\Delta E}\frac{xdx}{2(x+M^2)}\int d\tilde{\Omega}_k\frac{(p_i\cdot p_j)}{(p_i\cdot k)(p_j\cdot k)}$$
$$=4\pi(p_j\cdot p_j)\int_0^1\left\{\ln\frac{p_y^2}{\lambda^2}-2\ln\frac{(p_j\cdot t)}{M\eta\Delta E}-2\ln[1+y(p_i\cdot t-p_j\cdot t)/(p_j\cdot t)]\right\}\frac{dy}{p_y^2}$$
$$=4\pi K(p_i,p_j)-8\pi(p_i\cdot p_j)\ln\frac{(p_j\cdot t)}{M\eta\Delta E}\int_0^1\frac{dy}{p_y^2}-8\pi(p_i\cdot p_j)\int_0^1\frac{\ln[1+y(p_i\cdot t-p_j\cdot t)/(p_j\cdot t)]}{p_y^2}dy. \tag{III.21}$$

The first term is the infrared term and it cancels out completely with the similar term in the elastic scattering cross section. The integrations of the second and third terms are straightforward, the results are listed in Appendix B.

The observable cross section is obtained by adding elastic and inelastic scattering cross sections. We have

$$\frac{d\sigma}{d\Omega}=\left(\frac{d\sigma}{d\Omega}\right)_{\text{elastic}}+\left(\frac{d\sigma}{d\Omega}\right)_b\equiv\left(\frac{d\sigma}{d\Omega}\right)_{\text{Rosenbluth}}(1+\delta), \tag{III.22}$$

where

$$\delta=\frac{-\alpha}{\pi}\left\{\frac{28}{9}-\frac{13}{6}\ln\left(\frac{-q^2}{m^2}\right)+\left(\ln\frac{-q^2}{m^2}-1+2Z\ln\eta\right)\left(2\ln\frac{E_1}{\Delta E}-3\ln\eta\right)-\Phi\left(\frac{E_3-E_1}{E_3}\right)-Z^2\ln\frac{E_4}{M}\right.$$
$$+Z^2\ln\frac{M}{\eta\Delta E}\left(\frac{1}{\beta_4}\ln\frac{1+\beta_4}{1-\beta_4}-2\right)+\frac{Z^2}{\beta_4}\left[\frac{1}{2}\ln\frac{1+\beta_4}{1-\beta_4}\ln\frac{E_4+M}{2M}-\Phi\left(-\left(\frac{E_4-M}{E_4+M}\right)^{\frac{1}{2}}\left(\frac{1+\beta_4}{1-\beta_4}\right)^{\frac{1}{2}}\right)\right]$$
$$+Z\left[\Phi\left(-\frac{M-E_3}{E_1}\right)-\Phi\left(\frac{M(M-E_3)}{2E_3E_4-ME_1}\right)+\Phi\left(\frac{2E_3(M-E_3)}{2E_3E_4-ME_1}\right)+\ln\left|\frac{2E_3E_4-ME_1}{E_1(M-2E_3)}\right|\ln\left(\frac{M}{2E_3}\right)\right]$$
$$-Z\left[\Phi\left(-\frac{E_4-E_3}{E_3}\right)-\Phi\left(\frac{M(E_4-E_3)}{2E_1E_4-ME_3}\right)+\Phi\left(\frac{2E_1(E_4-E_3)}{2E_1E_4-ME_3}\right)+\ln\left|\frac{2E_1E_4-ME_3}{E_3(M-2E_1)}\right|\ln\left(\frac{M}{2E_1}\right)\right]$$
$$-Z\left[\Phi\left(-\frac{M-E_1}{E_1}\right)-\Phi\left(\frac{M-E_1}{E_1}\right)+\Phi\left(\frac{2(M-E_1)}{M}\right)+\ln\left|\frac{M}{2E_1-M}\right|\ln\left(\frac{M}{2E_1}\right)\right]$$
$$\left.+Z\left[\Phi\left(-\frac{M-E_3}{E_3}\right)-\Phi\left(\frac{M-E_3}{E_3}\right)+\Phi\left(\frac{2(M-E_3)}{M}\right)+\ln\left|\frac{M}{2E_3-M}\right|\ln\left(\frac{M}{2E_3}\right)\right]\right\}. \tag{III.23}$$

$\Phi(x)$ is the Spence function[18]

$$\Phi(x)=\int_0^x\frac{-\ln|1-y|\,dy}{y} \tag{III.24}$$

and β_4 is the ratio of the velocity of the recoil proton to that of light,

$$\beta_4=(E_4^2-M^2)^{\frac{1}{2}}/E_4,\quad E_4=E_1+M-E_3.$$

We have kept Z in our formula for convenience of discussion. Z is equal to $+1$ for e^-+p scattering and is equal to -1 for e^++p scattering. The terms proportional to Z come from the interference terms between

[18] K. Mitchell, Phil. Mag. 40, 351 (1949).

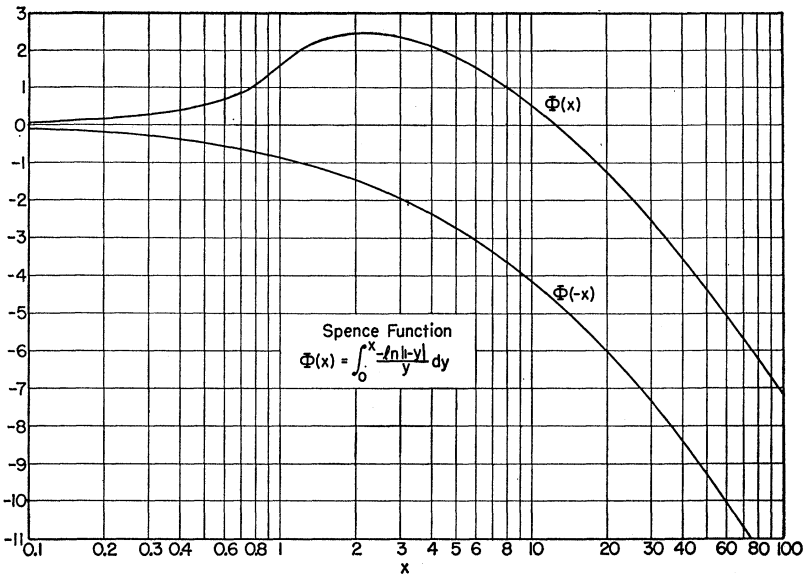

FIG. 5. Spence function $\Phi(x)$.

M_{b1} and M_{b2} and the terms proportional to Z^2 come from $M_{b2}^{\dagger}M_{b2}$. If we neglect the radiation from the proton current, i.e., letting $Z=0$ in Eq. (III.23), we obtain Eq. (I.4), except for a small term $\Phi[(E_3-E_1)/E_1]$, which we guessed on intuitive physical grounds. We notice that the radiation from the proton current increases (or decreases) the radiative corrections to e^-+p (or e^++p) scatterings.

IV. NUMERICAL EXAMPLES

Example A. Consider the radiative corrections under the following conditions[3]:

$E_1=900$ Mev, $\theta=145°$, $\eta=2.75$,

$E_3=327$ Mev, $E_4=1511$ Mev, $\Delta E=13.1$ Mev,

$\beta_4=0.783$ $q^2=-2M(E_1-E_3)=-1.075\times10^6$ Mev^2.

Equation (III.23) gives $\delta=-15\%$ for e^-+p and $\delta=-8.6\%$ for e^++p scatterings. If one neglects the radiation from protons, one gets from Eq. (I.4) $\delta=-11\%$.

Example B. Consider an example at a higher energy:

$E_1=5$ Bev, $E_3=500$ Mev, $\eta=10$, $\Delta E=10$ Mev, $\beta_4=0.975$.

Equation (III.23) gives $\delta=-21.0\%$ for e^-+p and $\delta=-9.9\%$ for e^++p scatterings. Equation (I.4) gives $\delta=-12.84\%$.

Notice in both examples given above that the condition (III.3) is satisfied.

V. PRACTICAL CONSIDERATIONS

In applying Eq. (III.23) to the actual analysis of data some precautions are necessary. When an electron beam is scattered by a liquid hydrogen target, the scattered electrons, after going through an entrance slit and the magnetic spectrometer, will have a typical energy spectrum shown in Fig. 1. The shape of this spectrum is in general due to (1) the energy spread of the incident beam, (2) the finite thickness of the target, (3) the finite width of the entrance slit, and (4) the radiative corrections which we have treated in this paper. The effect due to the finite thickness of the target is also a radiative phenomenon and thus one should be able to calculate it along lines similar to the present treatment. This effect may cause as much as 10% correction to the cross section at 900 Mev under typical experimental conditions.[19] The smearing of the energy spectrum due to the energy spread of the incident beam and the finite width of the entrance slit do not cause any appreciable trouble as long as ΔE is chosen sufficiently larger than the energy spread of the scattered electrons due to these two effects. Suppose the initial beam has an energy spread ΔE_1; then the energy spread of the scattered electron due to ΔE_1 can be calculated from Eq. (I.2):

$$(\partial E_3/\partial E_1)\Delta E_1=\Delta E_1\eta^{-2}. \tag{V.1}$$

Similarly the energy spread of E_3 due to the finite width of the entrance slit is

$$(\partial E_3/\partial\theta)\Delta\theta=(E_1^2/M\eta^2)\sin\theta d\theta. \tag{V.2}$$

Thus one should choose ΔE such that

$$\Delta E\gg\Delta E_1\eta^{-2}, \tag{a}$$

and

$$\Delta E>(E_3^2/M)\sin\theta\Delta\theta. \tag{b}$$

The condition (a) is necessary because the shape of the spectrum near $E_3^{el}(\theta_{av})$ is mainly due to the energy

[19] R. Hofstadter (private communication). See reference 6, Eq. (34). This formula needs a reexamination at energies with which we are concerned here.

spread of the incident beam, which has nothing to do with the radiative effect. Condition (b) is necessary because we have replaced the area of integration $ABCD$ by $AB'C'D$ in Fig. 4 in order to simplify the calculation. This approximation breaks down unless condition (b) is satisfied.[20] Experimentally these two conditions are equivalent to taking $\Delta E \gg W$, where W is the width of the spectrum to the right of $E_3^{el}(\theta_{av})$ as shown in Fig. 1.

Conditions (a) and (b) give a lower limit for ΔE. On the other hand ΔE should not be too large, otherwise condition (III.3) will not be satisfied.

VI. DISCUSSION

A. In this paper we have amply demonstrated the power of the technique of infrared extraction developed by Yennie *et al.*[8] We have assumed the noninfrared parts of the matrix elements M_2, M_3, and M_6 to be negligible. This has to be somehow justified. Drell and Fubini[7] have considered the mesonic contributions to M_2 and M_3, especially the resonance effect of the nucleon Compton scattering. They estimated the contribution on the cross section to be about 1% in the energy range $\sim$1 Bev. It is very desirable to extend this kind of consideration to higher energies.[21] One could of course try to treat the proton as a structureless Dirac particle and calculate these matrix elements exactly and show that the noninfrared parts are indeed negligible.[22] However, in an electron-electron scattering[9] it was explicitly shown that the noninfrared parts of M_2+M_3 are negligible. Thus one would expect that this must also be true for $e+p$ scattering if protons are structureless. The order of magnitude of the contribution to the cross section from M_6 can be estimated by using Eq. (II.5) with m^2 replaced by M^2. It can be shown that even at $E_1=10$ Bev, and $E_3=500$ Mev, the contribution to the cross section from M_6 is only about $+0.5\%$. Thus the neglect of the noninfrared parts of M_6 is probably justified up to about 10 Bev. In summary, our Eq. (III.23) is good up to about 1 Bev within $\pm 2\%$ of the cross section. (Of the 2% error, 1% is from the approximation used in our integration and 1% from the noninfrared parts of the contributions from $M_2+M_3+M_6$.) If one can prove that the noninfrared parts of M_2+M_3, especially the mesonic resonance effects, are negligible ($\pm 1\%$) even at higher energies, then our result is good up to about 5 Bev within 2% of the cross section.

B. In this paper we have considered the radiative corrections to the $e+p$ scattering when only the scattered electrons are detected. In part of the Cornell experiment[4] the recoil protons are detected instead of the scattered electrons. Our formula is not applicable under this experimental condition. Under this experimental condition, very hard photons can be emitted along the direction of the scattered electrons and thus one would expect the radiative corrections should be much smaller than the result of the present calculation.

VII. ACKNOWLEDGMENTS

The author is grateful to Professor S. D. Drell for suggestions and criticism of the manuscript. Discussions with Professor D. R. Yennie, Professor J. D. Bjorken, and Dr. S. C. Frautschi were helpful. The author wishes to express his thanks to Professor R. Hofstadter, Dr. E. B. Dally, and Dr. F. Bumiller for discussions on some experimental matters.

APPENDIX A

We have neglected the photon momentum k in the numerators of Eqs. (III. 1,2). We investigate here under what experimental conditions this procedure is justified. For this purpose it is necessary to consider everything in the center-of-mass system. (We denote the quantities in the c.m. system by a tilde in this section.) It is easily seen that for the above-mentioned approximation to be applicable, the maximum energy of a photon ω_{max} which can be emitted in the c.m. system must be smaller than the momentum of all the particles. Thus in the center-of-mass system,

$$\tilde{\omega}_{max} \ll \tilde{E}_1. \tag{A.1}$$

To determine the value of ω_{max} we transform experimental conditions as specified by Fig. 4 into those in the c.m. system. The result is plotted in Fig. 6. $\tilde{E}_1$ can be obtained by considering the invariant

$$p_1 \cdot p_2 = ME_1 \approx \tilde{E}_1\tilde{E}_2 + \tilde{E}_1^2 \approx \tilde{E}_1[(\tilde{E}_1^2+M^2)^{\frac{1}{2}}+\tilde{E}_1].$$

Hence

$$\tilde{E}_1 \approx E_1[1+(2E_1/M)]^{-\frac{1}{2}}. \tag{A.2}$$

Similarly,

$$\tilde{E}_2 \approx (E_1+M)[1+(2E_1/M)]^{-\frac{1}{2}}. \tag{A.3}$$

---

[20] In electron-electron scattering when one of the initial electrons is at rest, the extreme opposite condition to (*b*) was used. See reference 9, Sec. V.

[21] The noninfrared parts of M_2+M_3, including the mesonic effects, can be evaluated experimentally by comparing the cross sections of e^++p with those of e^-+p scatterings performed under identical experimental conditions. After applying the radiative corrections given by Eq. (III.23), the difference in two cross sections must be exactly twice the contributions from the noninfrared parts of M_2+M_3. (We assumed that the difference in the effects due to the finite target thickness for e^-+p and e^++p scatterings is negligible.) Such an experiment is being performed at Stanford by J. Pine and D. Yount.

[22] In this connection it is interesting to notice that McKinley and Feshbach have calculated the second Born approximation to the Coulomb scattering and found that the first Born cross section is altered by a factor $(1+\delta)$, where $\delta = Z\alpha\pi[\sin(\frac{1}{2}\theta)-\sin^2(\frac{1}{2}\theta)] \times\cos^{-2}(\frac{1}{2}\theta)$. In a later paper Dalitz confirmed this result. This correction is independent of energy and has different signs for e^-+p ($Z=1$) and e^++p ($Z=-1$) scatterings. At 145° this correction gives $\delta \approx 0.015Z$ and at smaller angles the correction is smaller. In view of the lack of exact calculation for the noninfrared parts of M_2+M_3, we may add this correction to Eq. (III.23) for practical analysis of the $e^\pm+p$ scatterings. See W. A. McKinley, Jr., and H. Feshbach, Phys. Rev. **74**, 1759 (1948); and R. H. Dalitz, Proc. Roy. Soc. (London) **A206**, 509 (1951).

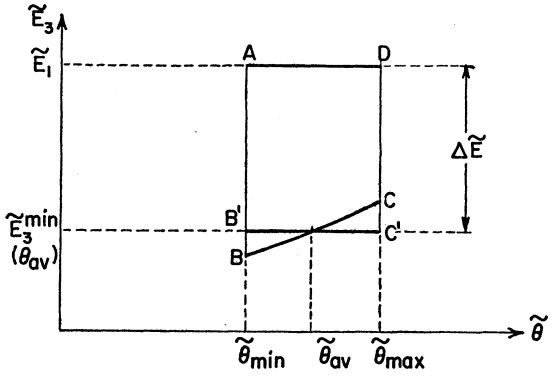

FIG. 6. Experimental conditions (Fig. 4) expressed in terms of quantities in the center-of-mass system.

For the elastic scattering, $\tilde{E}_3=\tilde{E}_1$, which corresponds to the straight line AD in Fig. 6. The lower bound of $\tilde{E}_3$ can be obtained by considering the invariant

$$p_3\cdot p_2=ME_3^{\min}\simeq\tilde{E}_3(\tilde{E}_2+\tilde{E}_1\cos\tilde{\theta}).$$

Hence,

$$\tilde{E}_3=ME_3^{\min}(\tilde{E}_2+\tilde{E}_1\cos\tilde{\theta})^{-1}, \tag{A.4}$$

which corresponds to the curve BC in Fig. 6. The relation between θ and $\tilde{\theta}$ can be obtained by considering the invariant

$$\frac{M^2(p_1\cdot p_3)}{(p_1\cdot p_2)(p_3\cdot p_2)}=(1-\cos\theta)=\frac{M^2(1-\cos\tilde{\theta})}{(\tilde{E}_1+\tilde{E}_2)(\tilde{E}_2+\tilde{E}_1\cos\tilde{\theta})}.$$

Hence,

$$\cos\tilde{\theta}=[(E_1+M)\cos\theta-E_1]\eta^{-1}M^{-1}, \tag{A.5}$$

and from this we obtain $\tilde{\theta}_{\min}$, $\tilde{\theta}_{av}$, and $\tilde{\theta}_{\max}$ corresponding, respectively, to $\theta_{\min}$, θ_{av}, and $\theta_{\max}$ of Fig. 4. Using an argument similar to that in the discussion of Fig. 4, we may replace the area $ABCD$ by the area $AB'C'D$. The length DC' is defined as $\Delta\tilde{E}$. Then from Eqs. (A.2, 3, 4, 5) we have

$$\begin{aligned}\Delta\tilde{E}&=\tilde{E}_1-ME_3^{\min}(\tilde{E}_2+\tilde{E}_1\cos\tilde{\theta}_{av})^{-1}\\&=\eta(1+2E_1M^{-1})^{-\frac{1}{2}}\Delta E.\end{aligned} \tag{A.6}$$

The maximum energy of a photon which can be emitted, $\omega_{\max}(\alpha,\varphi)$, can be calculated by using the equation $(p_1+p_2-p_3-k)^2=M^2$ and letting $\tilde{E}_3=\tilde{E}_3^{\min}$. We have then

$$\tilde{\omega}_{\max}(\alpha,\varphi)=\frac{\Delta\tilde{E}(M+2E_1)}{M+E_1+E_1(\cos\tilde{\theta}\cos\alpha+\sin\alpha\cos\varphi\sin\tilde{\theta})}, \tag{A.7}$$

where α and φ are defined in Fig. 7. If the photon $\tilde{k}$ is emitted along the direction of $\tilde{p}_1$, we have

$$\tilde{\omega}_{\max}(0,\varphi)=\Delta\tilde{E}\eta. \tag{A.8}$$

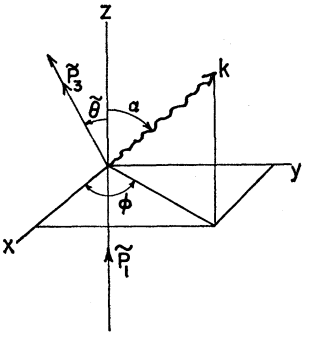

FIG. 7. The geometry for calculating the maximum energy of a photon which can be emitted in the center-of-mass system. p_3 is on the xz plane.

Similarly, along the $\tilde{p}_2$, $\tilde{p}_3$, and $\tilde{p}_4$ directions we have, respectively,

$$\tilde{\omega}_{\max}(\pi,\varphi)=\Delta\tilde{E}\frac{M+2E_1}{M+E_1(1-\cos\tilde{\theta})}$$

$$<\Delta\tilde{E}(1+2E_1M^{-1}), \tag{A.9}$$

$$\tilde{\omega}_{\max}(\tilde{\theta},0)=\Delta\tilde{E}, \tag{A.10}$$

and

$$\tilde{\omega}_{\max}(\pi-\theta,\pi)=\Delta\tilde{E}\frac{M+2E_1}{M+E_1\sin^2\tilde{\theta}}<\Delta\tilde{E}(1+2E_1M^{-1}). \tag{A.11}$$

From Eqs. (A.6, 8, 9, 10 and 11) we have

$$\tilde{\omega}_{\max}<\eta(1+2E_1M^{-1})^{\frac{1}{2}}\Delta E. \tag{A.12}$$

Thus condition (A.1) can be written in terms of lab quantities [using Eq. (A.2)] as

$$\Delta E(1+2E_1M^{-1})\ll E_3. \tag{III.3}$$

This result is very important experimentally. In example B of Sec. IV, the maximum energy of a photon which can be emitted along the p_1 direction is $\Delta E\eta^2=1$ Bev in the lab system. Our consideration here shows that even in this case the approximation we used is not bad.

APPENDIX B

We list here the results of all the integrations which appeared in Eq. (III.21). The invariant products $(p_i\cdot l)$ in Eq. (III.21) are reduced to lab quantities by using Eqs. (III.20). Let us define

$$I_{i,j}\equiv\frac{-1}{8\pi}\int_{2\lambda M}^{2M\eta\Delta E}\frac{xdx}{2(x+M^2)}\int d\tilde{\Omega}_k\frac{(p_i\cdot p_j)}{(p_i\cdot k)(p_j\cdot k)}$$

$$+\tfrac{1}{2}K(p,p_ip_j).$$

Then the following results can be obtained from Eq.

(III.21):

$$I_{1,1}=\ln\frac{E_1}{\eta^2\Delta E},\quad I_{2,2}=\ln\frac{E_4}{\eta\Delta E},$$

$$I_{3,3}=\ln\frac{E_3}{\Delta E},\quad I_{4,4}=\ln\frac{M}{\eta\Delta E},$$

$$2I_{1,3}=\left(\ln\frac{E_1}{\eta^2\Delta E}+\ln\frac{E_3}{\Delta E}\right)\ln\frac{-q^2}{m^2}-\Phi\left(\frac{E_3-E_1}{E_3}\right),$$

$$2I_{2,3}=\ln\frac{E_3}{\Delta E}\ln\frac{4E_3^2}{m^2}-\left[\Phi\left(-\frac{M-E_3}{E_1}\right)-\Phi\left(\frac{M(M-E_3)}{2E_3E_4-ME_1}\right)+\Phi\left(\frac{2E_3(M-E_3)}{2E_3E_4-ME_1}\right)+\ln\left|\frac{2E_3E_4-ME_1}{E_1(M-2E_3)}\right|\ln\frac{M}{2E_3}\right],$$

$$2I_{2,1}=\ln\frac{E_1}{\eta^2\Delta E}\ln\frac{4E_1^2}{m^2}-\left[\Phi\left(-\frac{E_4-E_3}{E_3}\right)-\Phi\left(\frac{M(E_4-E_3)}{2E_1E_4-ME_3}\right)+\Phi\left(\frac{2E_1(E_4-E_3)}{2E_1E_4-ME_3}\right)+\ln\left|\frac{2E_1E_4-ME_3}{E_3(M-2E_1)}\right|\ln\frac{M}{2E_1}\right],$$

$$2I_{4,1}=\ln\frac{E_1}{\eta^2\Delta E}\ln\frac{4E_3^2}{m^2}-\left[\Phi\left(-\frac{M-E_3}{E_3}\right)+\Phi\left(\frac{M-E_3}{E_3}\right)+\Phi\left(\frac{2(M-E_3)}{M}\right)+\ln\left|\frac{M}{2E_3-M}\right|\ln\frac{M}{2E_3}\right],$$

$$2I_{4,3}=\ln\frac{E_3}{\Delta E}\ln\frac{4E_1^2}{m^2}-\left[\Phi\left(-\frac{M-E_1}{E_1}\right)-\Phi\left(\frac{M-E_1}{E_1}\right)+\Phi\left(\frac{2(M-E_1)}{M}\right)+\ln\left|\frac{M}{2E_1-M}\right|\ln\frac{M}{2E_1}\right],$$

$$2I_{2,4}=\frac{1}{\beta_4}\ln\frac{1+\beta_4}{1-\beta_4}\ln\frac{M}{\eta\Delta E}+\frac{1}{\beta_4}\left[\frac{1}{2}\ln\frac{1+\beta_4}{1-\beta_4}\ln\frac{E_4+M}{M}-\Phi\left(-\left(\frac{E_4-M}{E_4+M}\right)^{\frac{1}{2}}\left(\frac{1+\beta_4}{1-\beta_4}\right)^{\frac{1}{2}}\right)\right].$$

The following identity was found to be useful in many of the above integrations:

$$\int_0^1\frac{\ln(1+cy)dy}{ay^2+by}=\frac{-1}{b}\left[\Phi(-c)-\Phi\left(\frac{a+b}{b-(a/c)}\right)+\Phi\left(\frac{1}{1-(a/bc)}\right)+\ln|(bc/a)-1|\ln\left(\frac{a+b}{b}\right)\right].$$